DOI: 10.1002/ejic.201101406

Complexation of Palladium(II) with Unsaturated Dithioethers – A Systematic Development of Highly Selective Ligands for Solvent Extraction[‡]

Juliane Traeger,[a] Tillmann Klamroth,[b] Alexandra Kelling,[a] Susanne Lubahn,[a] Ernst Cleve,[c] Wulfhard Mickler,[a] Matthias Heydenreich,[d] Holger Müller,[a] and Hans-Jürgen Holdt*[a]

Keywords: Renewable resources / Palladium / Chelates / Ligand design / S ligands

There is a demand for new and robust Pd^{II} extractants due to growing recycling rates. Chelating dithioethers are promising substances for solvent extraction as they form stable square-planar complexes with Pd^{II}. We have modified unsaturated dithioethers, which are known to coordinate Pd^{II}, and adapted them to the requirements of industrial practice. The ligands are analogues of 1,2-dithioethene with varying electron-withdrawing backbones and polar end-groups. The crystal structures of several ligands and their palladium complexes were determined as well as their electro- and photochemical properties, complex stability and behaviour in solution. Solvent extraction experiments showed the superiority of some of our ligands over conventionally used extractants in terms of their very fast reaction rates. With highly selective 1,2-bis(2-methoxyethylthio)benzene (**4**) it is possible to extract Pd^{II} from a highly acidic medium in the presence of other base and palladium-group metals.

Introduction

The recovery of platinum-group metals (PGMs) from secondary sources such as automotive catalysts has gained increasing importance, especially in countries without PGM mines.[1] As measured by annual demand, palladium is one of the most important PGMs. In industrial process streams, it occurs in the divalent oxidation state and forms chlorido complexes, of which the tetrachloridopalladate anion $[PdCl_4]^{2-}$ is the most common species. In industry, it is mainly extracted by solvent extraction with hydroxyoximes or long-chain thioethers through the formation of inner-sphere complexes.[2–4] Due to slow extraction rates, the equilibration times of such systems are quite long.[3,4] The equilibrium times can be reduced with the help of phase-transfer catalysts, such as amines in the case of β-hydroxyoximes,[4] but they decrease the selectivity towards other metals. In addition, when using long-chain thioethers, stripping the palladium from the organic phase is found to be difficult.[4] In the field of basic research, there are currently still great efforts being undertaken to find new extractants.[5] These cover a wide range of functional groups: oxygen-containing crown ethers,[5a] nitrogen- and sulfur-containing protic ionic liquids,[5b] quaternary phosphonium salts,[5c] urea derivatives,[5d] pyridinecarboxamides,[5e] thiourea derivatives,[5f] compounds that contain sulfide, sulfinyl and sulfonyl groups[5g] and imidazole[5h] and triazole[5i] substitution products. Yet for most, the separation of Pd^{II} from Pt^{IV} is not very effective.

Thioethers are widely known as soft donors that form complexes with a range of transition metals.[6] Dithioethers based on *cis*-1,2-dithioethene possess a rigid chelating unit, which perfectly meets the geometrical demand for the square-planar complexation of Pd^{II}.[7] Recently, Ananikov et al. have reported sulfur-containing alkenes and their Pd^{II} complexes.[8] However a general risk when dealing with thioethers is the possible oxidation of the sulfur atom, especially in PGM refining processes when brought into contact with an oxidising aqueous phase. It is noted that dihexyl sulfide can be oxidised to a sulfoxide and thereafter to a sulfone, which does not only consume the extracting agent, but also may impair the selectivity of the system.[9] On this account it is advisable to design ligands with reduced electron density on the sulfur atoms. This can be achieved by introducing electron-withdrawing groups, such as cyano groups, at the double bond or making the double bond part of an aromatic ring.

Studies of maleonitrile dithiocrown ethers have shown that they form stable Pd^{II} complexes and have also demon-

---

[‡] Patent application filed on August 22, 2011, EP11178303.1

[a] University of Potsdam, Institute of Chemistry, Department of Inorganic Chemistry,
Karl-Liebknecht-Straße 24–25, 14476 Potsdam, Germany
Fax: +49-331-977-5055
E-mail: holdt@uni-potsdam.de
[b] University of Potsdam, Institute of Chemistry, Department of Theoretical Chemistry,
Karl-Liebknecht-Straße 24–25, 14476 Potsdam, Germany
[c] Hochschule Niederrhein, Institute for Coatings and Surface Chemistry,
Frankenring 20, 47798 Krefeld, Germany
[d] University of Potsdam, Institute of Chemistry, Department of Analytical Chemistry,
Karl-Liebknecht-Straße 24–25, 14476 Potsdam, Germany

Supporting information for this article is available on the WWW under http://dx.doi.org/10.1002/ejic.201101406.

strated their potential to extract Pd^{II} with a good selectivity towards other soft metal ions.[10,11] Another important attribute is their high surface activity caused by the ether groups. However, because of their low synthetic yields, these compounds have never been used on a large scale for solvent extraction. As Pd^{II} is coordinated exocyclically through the two sulfur atoms, the steric design does not stringently need to contain macrocycles.

Hence the open-chain equivalents, which are easier to synthesise, are promising ligands to be utilised in industrial processes. Pd^{II} complexes of 1,2-bis(methylthio)maleonitrile,[12] 1,2-bis(methylthio)benzene[7,12,13] and 4-methyl-1,2-bis(methylthio)benzene[13] have been investigated, but the ligands themselves have not received any attention concerning their possible applicability in solvent extraction. As the complexation of the metal occurs at the interface or in the aqueous phase, it is important that the extractant used is not too nonpolar, otherwise it takes too long to establish the equilibrium.

The main goal of this work was to synthesise a number of unsaturated "open-chain" dithioethers **1**–**6** (Scheme 1) and to examine their potential to extract $[PdCl_4]^{2-}$ from streams originating from automotive catalysts. Our focus was to create new extracting agents for practical applications and not only laboratory examination. First and foremost, this requires a relatively simple one-pot synthesis, and the compounds must be robust as they will be used in the extraction cycle repeatedly. By varying the electron-withdrawing effect on the sulfur atoms, the oxidation potential of the extractant and the stability of the Pd^{II} complexes formed were influenced. To ensure a good interaction with the aqueous phase, 2-hydroxyethyl or 2-methoxyethyl groups were inserted. A comparison of the extraction kinetics of the new substances with two industrial ones, dihexyl sulfide[14] and Aloxime® 840,[15] demonstrated the advantage of these new extracting agents. Although the electron-withdrawing effect of the benzene and maleonitrile units make the sulfur atoms harder, it was shown that the selectivity for Pd^{II} over other metals that occur in automotive catalysts (some of which in much higher concentrations) is excellent.

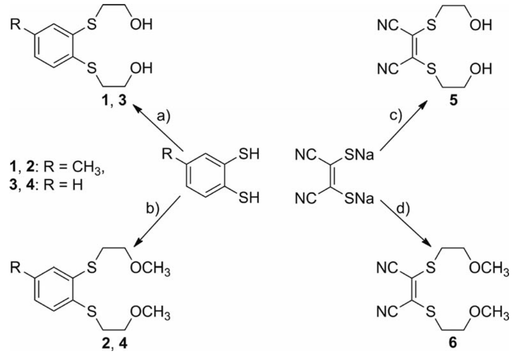

Scheme 1. Synthesis of the ligands: a) Na, $Br(CH_2)_2OH$, EtOH; b) Na, $Cl(CH_2)_2OCH_3$, EtOH; c) NaI, $Br(CH_2)_2OH$, acetone; d) NaI, $Cl(CH_2)_2OCH_3$, acetone.

Furthermore, we report the variable formation of complexes that depend on the concentration ratio (Pd^{II}/extractant). NMR spectroscopy and the single-crystal X-ray structures prove that an inversion of the sulfur and thus, oscillation of the arms occurred in solution. For a comprehensive understanding of the behaviour of an extractant, it is necessary to investigate the solid complex itself in addition to the processes that occur in solution. Theoretical calculations helped us to understand the electro- and photochemical characteristics of the extractants and their complexes.

Results and Discussion

Synthesis of the Ligands and their Complexes

We investigated a set of unsaturated dithioethers **1**–**6** (Scheme 1). The insertion of an unsaturated unit into a 4-methylbenzene (**1**, **2**) or benzene moiety (**3**, **4**) and the introduction of cyano groups at the double bond (**5**, **6**) increased the electron-withdrawing effect on the sulfur atoms. The benzene dithioethers **1**–**4** were synthesised by the addition of sodium to 4-methyl-1,2-benzenedithiol or 1,2-benzenedithiol[16] and the alkylation of the dithiolates formed with 2-bromoethanol or 2-chloroethyl methyl ether. The maleonitrile dithioethers **5** and **6** were prepared by the alkylation of disodium (*Z*)-1,2-dicyanoethene-1,2-dithiolate[17] with 2-bromoethanol and 2-chloroethyl methyl ether, respectively, in the presence of NaI following a procedure reported by Lange and coworkers.[18] We obtained single-crystal X-ray structures of **3**, **5** and **6**.[19] NMR spectroscopy and elementary analysis proved the purity of all our ligands. In contrast to other thioethers, these substances are not volatile and do not have the characteristic odour, which is important for practical applications. The complexes $[PdCl_2(L)]$ (L = **1**–**4**, **6**) were synthesised by a method similar to that described by Drexler et al.[10] The crystal structures of all of the Pd^{II} complexes were analysed, except for that containing **5**, which was an insoluble powder with an undefined composition.

Single-Crystal X-ray Structures

The single-crystal X-ray structures of **3** and **6** (Figure 1) indicate the preorganisation of the lone pairs of the sulfur atoms for the complexation of Pd^{II}. It is typical for dithioethers that contain a maleontrile[10] or *o*-benzene unit[20] that the S···S distance is less than the sum of the van der Waals radii, which is around 3.7 Å. The values for **3**, **5** and **6** are in agreement with this [2.984(1), 3.084(2) and 3.121(1) Å, respectively]. The molecular structures of $[PdCl_2(L)]$ (L = **1**–**4**, **6**) have planar five-membered chelate rings (Figures 2 and 4 show the structures of $[PdCl_2(\mathbf{6})]$ and $[PdCl_2(\mathbf{3})]$, respectively) with customary Pd–S bond lengths.[10,21] In the complexes that contain **1**–**4** and in that of **6**, the S···S distances increase to values between 3.17 and 3.19 Å. A comparison of dithioether **3**, which contains an *o*-benzene backbone, with the corresponding complex

[PdCl$_2$(**3**)] shows a slight extension of the C1–S1 and C2–S2 bonds by 0.02 Å and a shortening of the aromatic C1=C2 bond by 0.03 Å. In the complexation of **6**, which is the maleonitrile derivative, the changes in the C–S and double bond lengths are more pronounced. The C1–S1 and C2–S2 bond lengths are lengthened by 0.06 and 0.09 Å, respectively, and the C1=C2 distance is shortened by 0.1 Å. This is in accordance with a noticeable shift of the C=C vibrational band in the IR spectra. The band of the complex is shifted by 62 cm^{-1} compared to that of the free ligand, which is similar to the trend seen in the crystal structures and IR spectra of comparable maleonitrile dithiocrown ether complexes.[10]

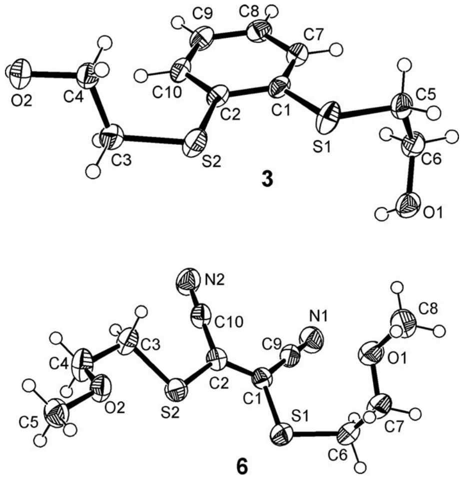

Figure 1. Molecular structures of **3** and **6** (thermal ellipsoids at 50%).

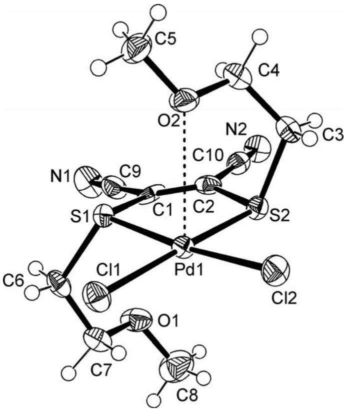

Figure 2. Molecular structure of [PdCl$_2$(**6**)] (thermal ellipsoids at 50%) showing the Pd···O2 interaction [2.918(4) Å].

Electrochemistry and DFT Calculations

The literature broadly describes that the oxidation of unsaturated thioethers leads to the formation of sulfones.[22] Oxidation generally occurs at the highest occupied molecular orbital (HOMO), hence DFT calculations were undertaken. We performed geometry optimisations for **3**, **6** and [PdCl$_2$(**3**)] using the Gaussian 09[23] program package at the CAM-B3LYP/LANL2DZ[24] level of theory. In addition, electrostatic potential (ESP)-derived charges[25] were calculated. In **3** and **6**, the electron density of the HOMO is mainly situated at the lone pair of the sulfur atoms and slightly at the double bond (**6**)[19] or the aromatic C=C bond adjacent to the sulfur atoms (**3**, Figure 3). Furthermore, the calculation of ESP charges of the cations confirms that oxidation takes place at the sulfur atom. Voltammetric data (Table 1) show that the introduction of electron-withdrawing groups significantly increases the oxidation potential of the unsaturated dithioethers in the following order: unsubstituted double bond [(*Z*)-1,2-bis(methylthio)ethene] < 4-methylbenzene backbone (**1**, **2**) < benzene backbone (**3**, **4**) << double bond with cyano groups (**5**, **6**). The oxidation potential of **5** and **6** is nearly twice that of the reference, (*Z*)-1,2-bis(methylthio)ethene[22b] (BMTE). Looking at the values of the Pd^{II} complexes of **1**–**4**, it is apparent that there is a significant enhancement of the oxidation potential caused by complexation. This is in line with the calculated HOMO energy levels of **3** and [PdCl$_2$(**3**)]. Compared to the ligand, the energy level of the complex is found at 0.17 eV lower values. The HOMO of the optimised structure of [PdCl$_2$(**3**)] is mainly situated at the chlorine atoms (Figure 3). In addition, a comparison of the ESP charges of the neutral complex with the corresponding cation reveals a shift of the partial negative charge at the PdCl$_2$ unit from –0.57 to –0.03 e. Therefore the oxidation of the PdCl$_2$ complexes that contain benzene dithioether ligands is believed to occur at the chlorine atoms and not at the sulfur atoms, whose electron density is further reduced by complexation. A noticeable difference is observed between the oxidation potentials of [PdCl$_2$(**1**)] and [PdCl$_2$(**3**)], which possess 2-hydroxyethyl end-groups at the two side arms, and [PdCl$_2$(**2**)] and [PdCl$_2$(**4**)], which contain 2-methoxyethyl end-groups. The values of the ligands do not differ in that way, which indicates the influence of the end groups on the electrochemical character of the palla-

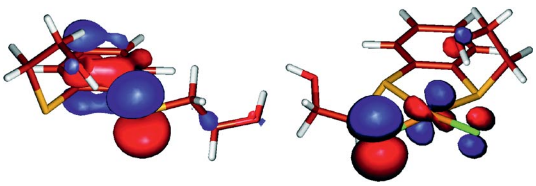

Figure 3. HOMOs of **3** and [PdCl$_2$(**3**)].

Table 1. Differential pulse voltammetry data for BMTE, **1**–**6** and [PdCl$_2$(L)] (L = **1**–**4**, **6**) in MeCN.[a]

Ligand	E_p^{Ox} [V][b]	E_p^{Red} [V][b]	Complex	E_p^{Ox} [V][b]	E_p^{Red} [V][b]
BMTE	+0.93	–			
1	+1.21	–	[PdCl$_2$(**1**)]	+1.63	–0.59
2	+1.22	–	[PdCl$_2$(**2**)]	+1.72	–0.67
3	+1.29	–	[PdCl$_2$(3)]	+1.62	–0.57
4	+1.29	–	[PdCl$_2$(**4**)]	+1.74	–0.62
5	+1.79	–1.06			
6	+1.84	–1.09	[PdCl$_2$(**6**)]	+1.81	–0.49

[a] All potentials are given vs. SCE. [b] Error ± 0.02 V.

dium complexes. This could be related to the weak Pd···O interaction (vide infra).

Electronic Spectra

The UV/Vis spectra of the unsaturated dithioethers **1**–**6** and the palladium complexes are in good agreement with the electrochemical data reported above as they confirm the electron-withdrawing character of the ligand backbones. In the spectra of **5** and **6**, the characteristic band of the dithiomaleonitrile push–pull π-electron system[26] is observed at 341 and 340 nm, respectively (see Figure 7 for the spectrum of **6**). This is caused by internal charge transfer from the sulfur atoms to the maleonitrile unit and is suppressed by the complexation of the sulfur atoms. The UV/Vis spectra of **1**–**4** are shaped by three bands that occur near 215, 247 and 300 nm (Figure 6, a). DFT calculations for **3**[19] imply that the band at 300 nm is induced by a HOMO–LUMO charge transfer from a sulfur atom to the aromatic ring. This is similar to the transfer known in the dithiomaleonitrile unit but occurs at a lower wavelength, denoting that the electron-withdrawing effect is smaller. The second transition is from HOMO-1, which is also dominated by the lone pair of a sulfur atom and energetically close to the HOMO, into the LUMO. The absorption near 215 nm is caused by the excitation from the HOMO to the π* orbital of the aromatic ring, which represents the LUMO+1. In the corresponding complex, [PdCl$_2$(**3**)], a small band at approximately 380 nm displays a d–d transition. A shoulder near 300 nm is caused by an excitation into the LUMO, which is situated at the metal.

Stereoisomerism of the Complexes in the Solid State and Solution

In thioether complexes, sulfur atoms can be centres of chirality. The Pd^{II} complexes synthesised with **1** and **2** are present in the *meso* form and those with **4** and **6** give a racemate. With **3**, the *meso* form and the racemate were obtained. To the best of our knowledge, [PdCl$_2$(**3**)] is the first palladium complex of an unsaturated 1,2-dithioether for which both diastereomeric forms could be isolated (Figure 4). The crystal structures of the racemic complexes show that one of the oxygen atoms is situated above the palladium at a distance that is slightly shorter than the sum of the van der Waals radii (3.1 Å)[27] (see the Supporting Information and Figure 2). For example, the distances in [PdCl$_2$(**3**)] and [PdCl$_2$(**6**)] are 3.058(3) and 2.918(4) Å, respectively. Thus a weak interaction of the oxygen atom with a d orbital of the palladium is possible. This is also indicated by the HOMO of the optimised structure [PdCl$_2$(**3**)] (Figure 3). In addition, a dispersion-driven hydrogen bond, as recently reported between water and Pt^{II},[28] could in principle be formed by the orientation of the OH proton towards the Pd centre. We see no indication for such bonding in the calculations, which is to be expected as dispersive interactions are not covered by the CAM-B3LYP functional. Nevertheless, the calculated Pd–O distance of 2.93 Å is in good agreement with that from the X-ray structure.

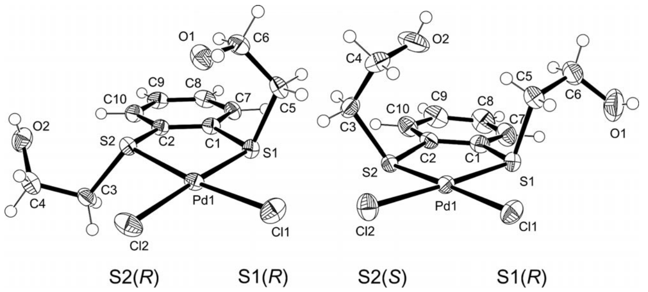

Figure 4. Molecular structures of (*R*,*R*)-[PdCl$_2$(**3**)] and (*S*,*R*)-[PdCl$_2$(**3**)] (thermal ellipsoids at 50%).

However, the two arms are very flexible in solution and can easily switch between the diastereomic forms. Based on ^{1}H NMR spectroscopic data, Abel et al. postulated a pyramidal inversion at sulfur in dithioether complexes of Pd^{II} in solution.[12,29] At low temperatures, they observed signals from two diastereomers – *meso* and DL – which, on warming, coalesced to time-averaged bands. Interestingly, although we dissolved the isolated isomers, we found the same (Table 2). For dichlorido[1,2-bis(2-methylthio)benzene]palladium(II), Abel et al. determined a coalescence temperature of –45 °C and computed an energy barrier of ca. 50 kJ/mol. The coalescence of the signals of [PdCl$_2$(**2**)] and [PdCl$_2$(**4**)] occurred between –60 and –30 °C, which suggests that the energy barrier is in the same magnitude as that of dichlorido[1,2-bis(2-methylthio)benzene]palladium(II). The other complexes were only poorly soluble in dichloromethane and gave no spectra worthy of evaluation. The diastereomers found at low temperatures are present in unequal abundance with an approximate ratio of 1:4. According to the study mentioned above, the racemate (*anti* conformation) predominates on account of its higher thermodynamic stability. From the number of peaks in the ^{13}C NMR spectrum of [PdCl$_2$(**4**)] (Table 2), it was seen that

Table 2. ^{13}C NMR chemical shifts [ppm] in CD$_2$Cl$_2$ for **2**, **4** (25 °C), [PdCl$_2$(**2**)] and [PdCl$_2$(**4**)] in two diastereomeric forms (–60 °C).

	2	[PdCl$_2$(**2**)][a]	[PdCl$_2$(**2**)][b]	**4**	[PdCl$_2$(**4**)][a]	[PdCl$_2$(**4**)][b]
S*C*=CS	137.4, 132.7	135.2, 132.5	135.1, 133.0	137.1	135.4	135.3
CH$_2$*C*H$_2$O	71.2, 71.1	69.5, 69.4	68.2, 68.2	71.0	69.7	68.4
O*C*H$_3$	58.7, 58.6	58.4, 58.4	58.1, 58.0	58.7	58.4	58.1
S*C*H$_2$CH$_2$	33.4, 32.8	42.7, 42.4	44.1, 43.7	32.9	42.9	44.1
*C*H$_3$C	21.0	20.6	20.6	–	–	–

[a] Major species. [b] Minor species.

both diastereomers retain σ and C_2 symmetry, respectively. The ^{1}H NMR spectrum of [PdCl$_2$(**4**)] exhibits a lot of overlaps in the range of the SCH_2CH$_2$ and CH$_2$$CH_2$O protons. Nonetheless, it can be seen from the heteronuclear single quantum coherence (HSQC) NMR spectrum (Figure 5) that the respective SCH_2CH$_2$ and CH$_2$$CH_2$O protons on the two arms are no longer magnetically equivalent – SCH$_2$CH$_2$ and CH$_2$$CH_2$O each give two coupling signals that each relate to two protons. The spectra of asymmetric [PdCl$_2$(**2**)][19] support this conclusion. Compared to the carbon resonances of the free ligands, in particular those of SCH$_2$CH$_2$ are extremely downfield shifted in [PdCl$_2$(**2**)] and [PdCl$_2$(**4**)]. These changes are more pronounced than those observed by Drexler at al. for palladium complexes with maleonitrile dithiocrown ethers,[10] which indicates the higher complex stability of the aromatic open-chain dithioether complexes.

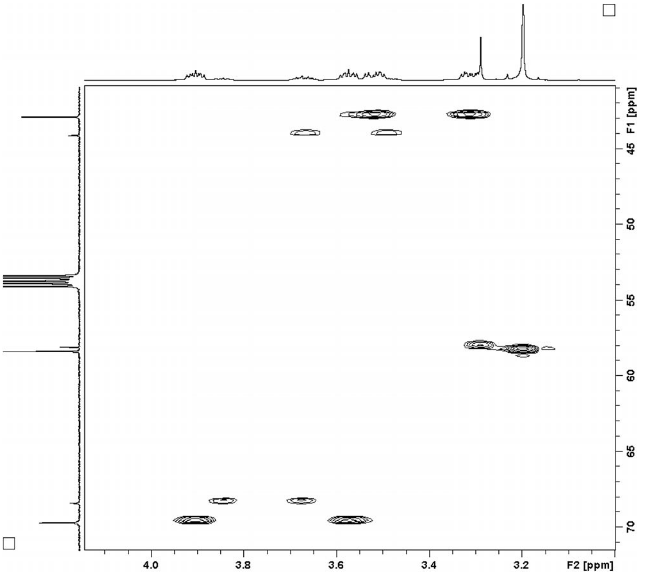

Figure 5. Aliphatic region of the HSQC NMR spectrum of [PdCl$_2$(**4**)] in CD$_2$Cl$_2$ at –60 °C showing the two diastereomeric species (*meso* and racemate).

Complex Stability Constants

With the help of UV/Vis titration experiments, the stability constants of the Pd^{II} complexes of **1**–**4** and **6** were determined (Table 3). The titrations were also adjuvant to observe the progress of complex formation. Because complexation is assumed to take place in the aqueous phase or interface in solvent extraction, water was chosen as solvent for all UV/Vis measurements. Figure 6 shows the titration curve of **3** as an example of **1**–**4**. With excess ligand, the reaction involves a species with a 1:2 (Pd:L) composition. In the presence of a higher metal concentration, this species degrades and forms the more stable [PdX$_2$(L)] complex. Derivative **6** just gives the complex with a 1:1 (Pd:L) composition (Figure 7), and the titration spectra show an isosbestic point.

Table 3. Complex stability constants determined by UV/Vis titration for [PdX$_2$(L)] and [Pd(L)$_2$]$^{2+}$ (L = **1**–**4** and **6**) in water (X = Cl$^-$, H$_2$O).

L	$\log K_{[\mathrm{PdX_2(L)}]}$	$\log K_{[\mathrm{Pd(L)_2}]^{2+}}$
1	$7.98 \pm < 0.01$	5.81 ± 0.01
2	$6.01 \pm < 0.01$	$5.65 \pm < 0.01$
3	7.99 ± 0.03	5.01 ± 0.02
4	5.97 ± 0.12	4.67 ± 0.02
6	4.74 ± 0.09	–

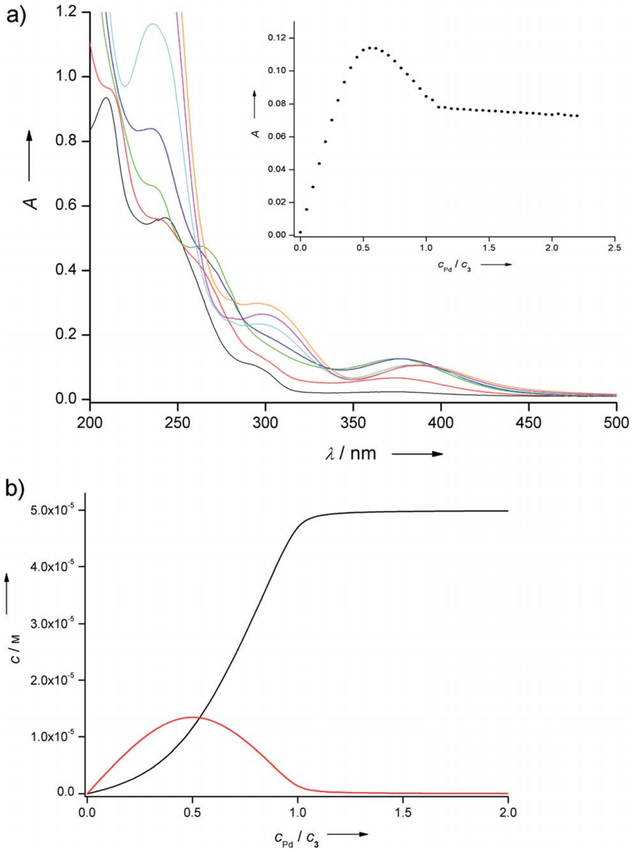

Figure 6. a) UV/Vis absorption spectra of **3** [c_0(**3**) = 5×10^{-5} M] in the presence of 0.0 (black), 0.2 (red), 0.5 (green), 0.7 (blue), 1.0 (cyan), 1.5 (magenta) and 2.0 equiv. (orange) of Pd^{II} in H$_2$O. Inset: titration curve at 375 nm. b) Calculated distribution of [Pd(**3**)$_2$]$^{2+}$ (red) and [PdCl$_2$(**3**)] (black) at various palladium/ligand ratios.

In compliance with the extraction results described below, the stability constant of [PdCl$_2$(**6**)] is much smaller than that of [PdX$_2$(L)] (L = **1**–**4**). This can be attributed to the higher electron density on the sulfur atoms in the benzene dithioethers **1**–**4** in comparison to the maleontrile dithioether **6**, which has already been shown by the lower oxidation potential of the aromatic compounds. The value is also smaller than the log *K* value of the comparable crown ether complex,[11] which is believed to be caused by the higher loss of entropy of the open-chain derivative in the course of complexation. The type of end group has a considerable influence on the $\log K_{[\mathrm{PdX_2(L)}]}$ values of the aromatic compounds. Complexes with 2-hydroxyethyl endgroups are more stable in water than those with 2-methoxy-

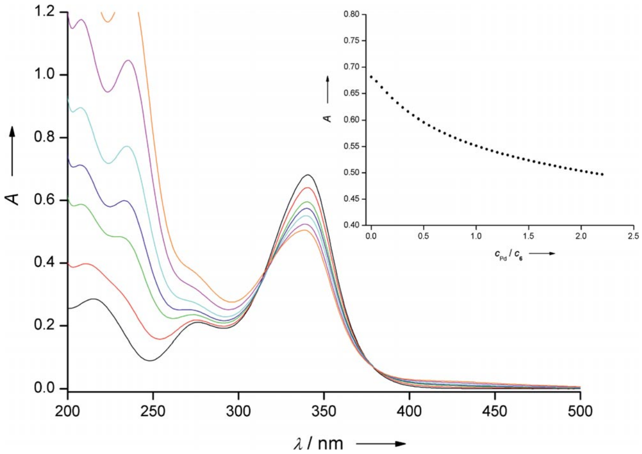

Figure 7. UV/Vis absorption spectra of **6** [$c_0(\mathbf{6}) = 5\times10^{-5}$ M] in the presence of 0.0 (black), 0.2 (red), 0.5 (green), 0.7 (blue), 1.0 (cyan), 1.5 (magenta) and 2.0 equiv. (orange) of Pd^{2+} in H_2O. Inset: titration curve at 340 nm.

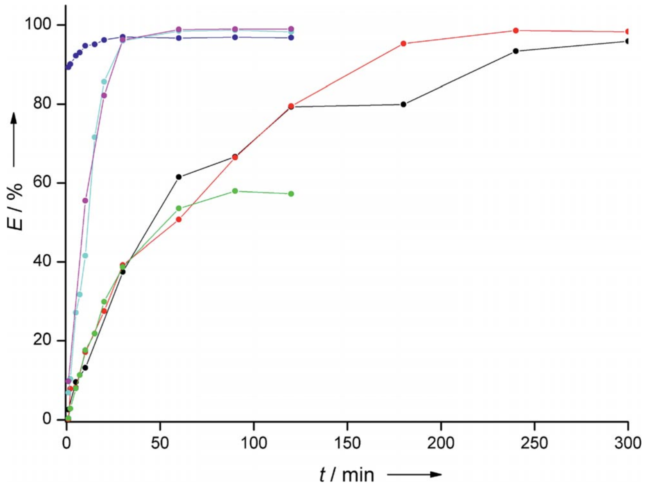

Figure 8. Solvent extraction kinetics of **2** (magenta), **4** (cyan), **5** (blue), **6** (green), dihexyl sulfide (red) and Aloxime® 840 (black) in $CHCl_3/H_2O$ = 1:1 [$c(L)_o = 10^{-2}$ M, $c_0(Pd)_w = 10^{-4}$ M, $c(Cl)_w = 1.5\times10^{-2}$ M]. The extraction yield, E, was determined by measuring $c(Pd)_w$ with inductively coupled plasma optical emission spectrometry (ICP OES).

ethyl groups. The $\log K_{[Pd(L)_2]^{2+}}$ values decrease in the order: $[Pd(\mathbf{1})_2]^{2+} > [Pd(\mathbf{2})_2]^{2+} > [Pd(\mathbf{3})_2]^{2+} > [Pd(\mathbf{4})_2]^{2+}$. Again, compared to ether end-groups, a hydroxy functionality enhances the complex stability in water. Complexes that possess a 4-methylbenzene backbone are more stable than those that contain a benzene backbone.

Solvent Extraction

We performed solvent extraction batch experiments with the unsaturated dithioethers **1**–**6** and various reference compounds. All tests were carried out in a chloroform/water system, where the extractant was present in excess in the organic phase. The composition of the aqueous phase, which contained Pd^{II}, was progressively modified from a model solution closer to industrial conditions. Figure 8 demonstrates the ability of **2**, **4** and **6** to transfer Pd^{II} from the aqueous into the organic phase. Compared to the two industrially used extractants, dihexyl sulfide[14] and Aloxime® 840,[15] all of our ligands that contain 2-methoxyethyl end-groups establish the extraction equilibrium extremely fast. In particular, **2** and **4**, which show extraction yields near 100% within only 30 min, are very promising new extractants. Ligand **5** formed an insoluble precipitate, which accumulated between the phases and could not be analysed. Thus, although the palladium content of the aqueous phase instantly dropped after contact with **5**, it is unsuitable as an extractant. Surprisingly, **1** and **3** did not extract any Pd^{II}. This was caused by their high water solubility, revealed by analysing both phases with UV/Vis spectroscopy. Both ligands form palladium complexes, but under the conditions chosen, their concentration in the aqueous phase was high enough to keep the palladium there.

Figure 9 shows the influence of the end groups on the extraction kinetics within a series of 1,2-dithio-4-methylbenzene derivatives. Acyclic **2** was tested in comparison to its crown ether analogue, 4-methylbenzodithio-12-crown-4,[30] and nonpolar, acyclic 1,2-bis(methylthio)-4-methylbenzene.[13] All of them exhibit very good extraction yields, but the time taken to reach the extraction equilibrium differed widely. The extraction took the longest with nonpolar 1,2-bis(methylthio)-4-methylbenzene. The reaction rate increases according an enhancement of the surface activity in the order of: methyl < 2-methoxyethyl group. 4-Methylbenzodithio-12-crown-4, which possesses a similar polarity to **2**, reacted the fastest. This difference in kinetics can be explained by the rigidity of the crown ether. Compared to open-chain **2**, it features better preorganisation for the complexation of Pd^{II}. Interestingly the extraction yield of **6** is less than that of **2** and **4**. This correlates with the order of the stability constants of their 1:1 Pd^{II} complexes. UV/Vis spectroscopy has shown that chlorido aqua Pd^{II} complexes exist in aqueous media with low chloride concentrations.[31] Water is a relatively weak electron donor and can be substituted more easily than chloride. Consequently, with an increase of the Cl^- concentration, $[PdCl_4]^{2-}$ becomes the prevailing species. For media that contain a high concentration of hydrochloric acid, such as the streams in PGM refining industries, the extractants used have to be strong enough to compete with Cl^- for the complexation of Pd^{II}. As seen from Figure 10, there is a huge difference in the extraction performance between **2**, **4** and **6**. The extraction yield of **6** dramatically decreases even on the addition of very small quantities of HCl. At a concentration of 0.26 M HCl, **6** extracts almost no Pd^{II} at all. The same trend is observed with the corresponding crown ether maleonitriledithio-12-crown-4,[32] although it is shifted to higher HCl concentrations. As it is more preorganised, the crown ether is a stronger chelating agent than open-chain **6**. However, utilising HCl concentrations higher than 1 M also depressed the extraction yield to negligible values. In contrast, **2** and **4** constantly exhibit extraction yields near 100% even at extremely high HCl concentrations. This is in accord with their higher complex stability constants.

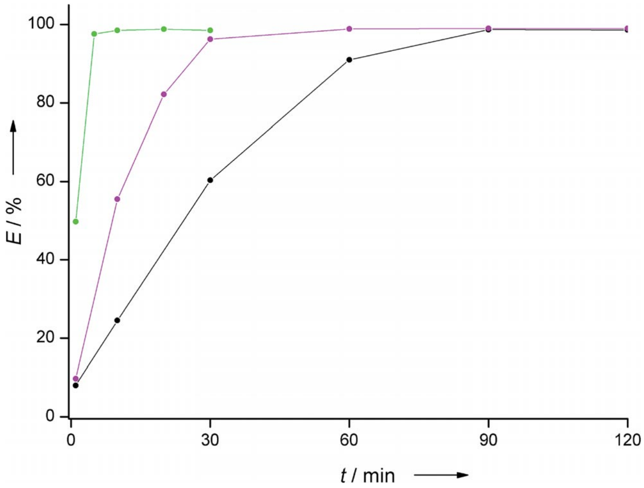

Figure 9. Solvent extraction kinetics of **2** (magenta), 4-methylbenzodithio-12-crown-4 (green) and 1,2-bis(methylthio)-4-methylbenzene (black) in $CHCl_3/H_2O$ = 1:1 [$c(L)_0 = 10^{-2}$ M, $c_0(Pd)_w = 10^{-4}$ M, $c(Cl)_w = 1.5 \times 10^{-2}$ M]. *E* was determined by measuring $c(Pd)_w$ with ICP OES.

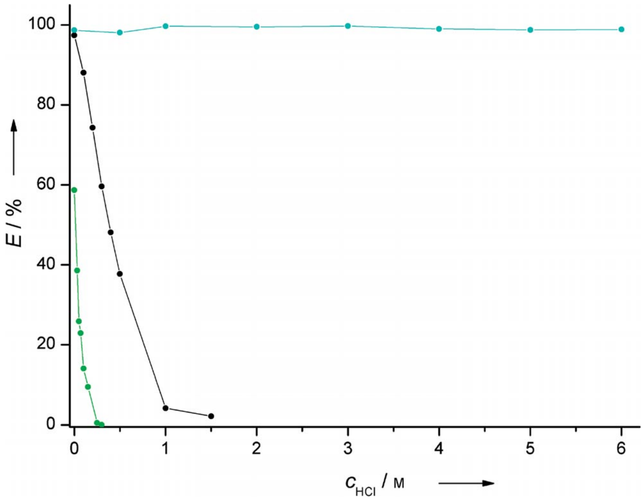

Figure 10. Dependency of the *E* value of maleonitriledithio-12-crown-4 (black), **2** (red), **4** (cyan) and **6** (green) on the HCl concentration added to the aqueous phase [$CHCl_3/H_2O$ = 1:1, $c(L)_0 = 10^{-2}$ M, $c_0(Pd)_w = 10^{-4}$ M, $c_0(Cl)_w = 1.5 \times 10^{-2}$ M]. *E* was determined by measuring $c(Pd)_w$ with ICP OES.

Figure 11 demonstrates the capability of **4** under conditions close to praxis. We extracted a solution, which was obtained by leaching an automotive catalyst with aqua regia followed by 1:1 dilution with water. In addition to an HCl concentration of nearly 4.5 M, this solution did not only contain a higher concentration of Pd^{II} but also Pt^{IV} and Rh^{III}, as well as a number of base metals, partially in 10-fold excess. The selectivity of **4** was found to be excellent. The organic phase contained 133 mg/L palladium, whereas the concentration of all the other metals was smaller than 0.2 mg/L. This experiment also demonstrates the redox stability of the system under strongly oxidising conditions.

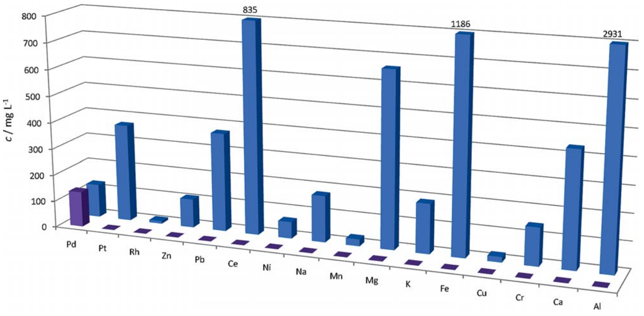

Figure 11. Solvent extraction batch experiment with a solution obtained by leaching an automotive catalyst with aqua regia (subsequent dilution with the same volume of water) and **4** in chloroform. The composition of the feed solution (blue) and organic phase (purple) was determined with ICP OES [$c(\mathbf{4})_0 = 10^{-2}$ M, $H_2O/CHCl_3$ = 1:1].

Conclusions

A new series of chelating ligands for the selective coordination of Pd^{II}, based on dithiomaleonitrile, dithiobenzene and dithiotoluene, has been designed and synthesised. They have a simple one-pot synthesis and a high stability towards oxidation, which makes them interesting for applications in solvent-extraction industries. The varying electron-withdrawing effect of the backbones does not only influence the electrochemical properties, as shown by the voltammetric measurements, UV/Vis spectra and DFT calculations, but also the complex stability and the kind of complex formed in solution. The dithiomaleonitrile-based compounds are weaker ligands and form only 1:1 (Pd:L) complexes, whereas aromatic **1**–**4** also build species of 1:2 composition.

In batch experiments, **2** and **4** particularly showed the capability to be used as solvent extractants. They are based on 1,2-dithio-4-methylbenzene and *o*-dithiobenzene, respectively, and contain 2-methoxyethyl arms. It was shown that the control of the polarity by the end groups had a big impact on the equilibrium times. Compared to conventionally used extractants such as dihexyl sulfide or hydroximes, our ligands had drastically increased reaction rates. The influence of varying the backbones of our ligands on the complex stability is reflected in a dramatic disparity of the extraction performance in the presence of chloride.

For an application in industry, it is important that the extractant is cheap to produce, very stable against oxidation and able to extract Pd^{II} from a medium that has a high hydrochloric acid content. On the other hand, the complex formed should not be too stable to enable fast elution. These criteria are perfectly met by **4**, which renders it the extractant of choice. We demonstrated the high potential of **4** by selectively extracting Pd^{II} from a solution of a leached automotive catalyst, which also contained a high concentration of other PGMs, base metals and hydrochloric acid.

Experimental Section

General: All reactions were carried out in dry solvents under an argon atmosphere. Melting points (m.p.) were measured with a capillary. NMR spectra of **1**–**6** were recorded with a Bruker Avance-300 spectrometer. The ^{1}H NMR chemical shifts are reported relative to the signal of $\mathrm{Me_4Si}$ (δ = 0 ppm) and the ^{13}C NMR chemical shifts relative to the solvent signal of $\mathrm{CDCl_3}$ (δ = 77 ppm). The assignments of the NMR signals were confirmed by 2D HMBC and HMQC NMR experiments. IR spectra were recorded with a Thermo Nicolet NEXUS FTIR instrument. UV/Vis spectroscopic measurements were performed with a Perkin–Elmer Lambda 950 spectrophotometer using quartz cuvettes. The EI MS spectra were recorded using a Thermo Quest SSQ 710 spectrometer. HRMS spectra of the complexes were measured with an Agilent 1200 series HPLC coupled with a 6210 ESI-TOF-MS using electrospray ionisation. Elemental analyses (C, H, N, S) of **1**–**6** were performed with an Elementar Vario EL elemental analyser and those of the complexes with an Elementar Vario Micro Cube and Thermo Finnigan EA 1112 series elemental analyser. The Pd content of $[\mathrm{PdCl_2(L)}]$ was determined by diluting the complex (1 mg) in 65% $\mathrm{HNO_3}$ (1 mL) and measuring with an Optima 5300 DV ICP OES instrument from Perkin–Elmer (λ = 340.458 nm).

General Procedure for the Synthesis of 1–4: Benzene-1,2-dithiol or toluene-3,4-dithiol (9.5 mmol) in ethanol (3 mL) was added to a solution of sodium (20 mmol) in ethanol (21 mL). The resulting solution was heated under reflux, and 2-bromoethanol or 2-chloroethyl methyl ether (20 mmol) was added. The solution was stirred under reflux for 15 h. The precipitate was removed, and the solvent was evaporated. The yellow, oily residue was purified by column chromatography on silica gel using chloroform as an eluent to afford **1**, **2** and **4** as colourless oils and **3** as white crystals.

1,2-Bis(2-hydroxyethylthio)-4-methylbenzene (1): Yield: 2.16 g (93%); R_f = 0.12 ($\mathrm{CHCl_3}$); $n_\mathrm{D}{}^{20}$ = 1.621. ^{1}H NMR (300 MHz, $\mathrm{CDCl_3}$, 25 °C, $\mathrm{Me_4Si}$): δ = 7.32 [d, ^3J(H,H) = 8 Hz, 1 H, $\mathrm{CHC}H\mathrm{CS}$], 7.21 (s, 1 H, $\mathrm{CC}H\mathrm{CS}$), 7.01 [d, ^3J(H,H) = 8.0 Hz, 1 H, $\mathrm{CC}H\mathrm{CH}$], 3.73 [t, ^3J(H,H) = 5.7 Hz, 2 H, $\mathrm{CH_2C^h}H_2\mathrm{O}$], 3.67 [t, ^3J(H,H) = 5.7 Hz, 2 H, $\mathrm{CH_2C^j}H_2\mathrm{O}$], 3.12 [t, ^3J(H,H) = 5.7 Hz, 2 H, $\mathrm{SC^g}H_2\mathrm{CH_2}$], 3.07 [t, ^3J(H,H) = 5.7 Hz, 2 H, $\mathrm{SC^i}H_2\mathrm{CH_2}$], 2.65 (br. s, 2 H, $\mathrm{O}H$), 2.32 (s, 3 H, $\mathrm{C}H_3\mathrm{C}$) ppm. ^{13}C NMR (75 MHz, $\mathrm{CDCl_3}$, 25 °C, $\mathrm{Me_4Si}$): δ = 138.1 ($\mathrm{CH_3}C\mathrm{CH}$), 137.5 ($\mathrm{CH}C^a\mathrm{S}$), 132.5 ($\mathrm{CH}C^f\mathrm{S}$), 132.1 ($\mathrm{CH}C\mathrm{HCS}$), 131.1 ($\mathrm{C}C\mathrm{HCS}$), 128.4 ($\mathrm{C}C\mathrm{HCH}$), 60.0 ($\mathrm{CH_2}C^h\mathrm{H_2O}$), 59.8 ($\mathrm{CH_2}C^j\mathrm{H_2O}$), 38.5 ($\mathrm{S}C^g\mathrm{H_2CH_2}$), 37.7 ($\mathrm{S}C^i\mathrm{H_2CH_2}$), 21.0 ($C\mathrm{H_3C}$) ppm. IR (KBr): $\tilde{\nu}$ = 3383 (O–H), 2921 (C–H), 2873 (C–H), 1459 (C–C), 1063 (C–OH), 1039 (C–OH), 1012 (C–OH) cm^{-1}. UV/Vis ($\mathrm{H_2O}$): $\lambda_{(\mathrm{max})}$ (ε, mol^{-1} dcm^{-1}) = 296 (1720), 247 (11704), 216 (22061) nm. MS (70 eV): *m*/*z* (%) = 244 (45) $[\mathrm{M}]^+$, 200 (75) $[\mathrm{C_9H_{12}OS_2}]^+$, 167 (100) $[\mathrm{C_9H_{11}OS}]^+$, 91 (65) $[\mathrm{C_7H_7}]^+$. $\mathrm{C_{11}H_{16}O_2S_2}$ (244.37): calcd. C 53.97, H 6.60, S 26.24; found C 54.01, H 6.57, S 26.08.

1,2-Bis(2-methoxyethylthio)-4-methylbenzene (2): Yield: 2.38 g (92%); R_f = 0.80 ($\mathrm{CHCl_3}$); $n_\mathrm{D}{}^{20}$ = 1.575. ^{1}H NMR (300 MHz, $\mathrm{CDCl_3}$, 25 °C, $\mathrm{Me_4Si}$): δ = 7.26 [d, ^3J(H,H) = 7.9 Hz, 1 H, $\mathrm{CHC}H\mathrm{CS}$], 7.13 (s, 1 H, $\mathrm{CC}H\mathrm{CS}$), 6.96 [d, ^3J(H,H) = 7.9 Hz, 1 H, $\mathrm{CC}H\mathrm{CH}$], 3.53–3.63 (m, 4 H, $\mathrm{CH_2C^{j,h}}H_2\mathrm{O}$), 3.38 (s, 3 H, $\mathrm{OC^l}H_3$), 3.35 (s, 3 H, $\mathrm{OC^m}H_3$), 3.04–3.13 (m, 4 H, $\mathrm{SC^{i,\,g}}H_2\mathrm{CH_2}$), 2.31 (s, 3 H, $\mathrm{C}H_3\mathrm{C}$) ppm. ^{13}C NMR (75 MHz, $\mathrm{CDCl_3}$, 25 °C, $\mathrm{Me_4Si}$): δ = 137.7 ($\mathrm{CH_3}C\mathrm{CH}$), 137.2 ($\mathrm{CH}C^a\mathrm{S}$), 132.5 ($\mathrm{CH}C^f\mathrm{S}$), 130.9 ($\mathrm{CH}C\mathrm{HCS}$), 129.6 ($\mathrm{C}C\mathrm{HCS}$), 127.3 ($\mathrm{C}C\mathrm{HCH}$), 71.0 ($\mathrm{CH_2}C^h\mathrm{H_2O}$), 70.9 ($\mathrm{CH_2}C^j\mathrm{H_2O}$), 58.7 ($\mathrm{O}C^l\mathrm{H_3}$), 58.6 ($\mathrm{O}C^m\mathrm{H_3}$), 33.2 ($\mathrm{S}C^g\mathrm{H_2CH_2}$), 32.5 ($\mathrm{S}C^i\mathrm{H_2CH_2}$), 21.0 ($C\mathrm{H_3C}$) ppm. IR (KBr): $\tilde{\nu}$ = 2980 (C–H), 2924 (C–H), 2876 (C–H), 2823 (C–H), 2808 (C–H), 1459 (C–C), 1114 (C–O), 1095 (C–O), 1040 (C–O) cm^{-1}. UV/Vis ($\mathrm{H_2O}$): $\lambda_{(\mathrm{max})}$ (ε, mol^{-1} dcm^{-1}) = 298 (1927), 248 (10224), 216 (18856) nm. MS (70 eV): *m*/*z* (%) = 272 (43) $[\mathrm{M}]^+$, 214 (36) $[\mathrm{C_{10}H_{14}OS_2}]^+$, 167 (100) $[\mathrm{C_9H_{11}OS}]^+$, 91 (65) $[\mathrm{C_7H_7}]^+$. $\mathrm{C_{13}H_{20}O_2S_2}$ (272.42): calcd. C 57.32, H 7.40, S 23.54; found C 57.11, H 7.45, S 23.64.

1,2-Bis(2-hydroxyethylthio)benzene (3): Yield: 2.19 g (94%); R_f = 0.11 ($\mathrm{CHCl_3}$); m.p. 84.5–86.0 °C. ^{1}H NMR (300 MHz, $\mathrm{CDCl_3}$, 25 °C, $\mathrm{Me_4Si}$): δ = 7.38–7.43 (m, 2 H, $\mathrm{CHC}H\mathrm{CS}$), 7.18–7.24 (m, 2 H, $\mathrm{CHC}H\mathrm{CH}$), 3.72 [t, ^3J(H,H) = 5.7 Hz, 4 H, $\mathrm{CH_2C}H_2\mathrm{O}$], 3.12 [t, ^3J(H,H) = 5.7 Hz, 4 H, $\mathrm{SC}H_2\mathrm{CH_2}$], 2.58 (s, 2 H, $\mathrm{O}H$) ppm. ^{13}C NMR (75 MHz, $\mathrm{CDCl_3}$, 25 °C, $\mathrm{Me_4Si}$): δ = 136.8 ($\mathrm{CH}C\mathrm{S}$), 130.9 ($\mathrm{CH}C\mathrm{HCS}$), 127.5 ($\mathrm{CH}C\mathrm{HCH}$), 59.9 ($\mathrm{CH_2}C\mathrm{H_2O}$), 37.8 ($\mathrm{S}C\mathrm{H_2CH_2}$) ppm. IR (KBr): $\tilde{\nu}$ = 3329 (O–H), 3250 (O–H), 2971 (C–H), 2954 (C–H), 2923 (C–H), 2873 (C–H), 1449 (C–C), 1057 (C–OH), 1039 (C–OH), 1023 (C–OH), 1008 (C–OH) cm^{-1}. UV/Vis ($\mathrm{H_2O}$): $\lambda_{(\mathrm{max})}$ (ε, mol^{-1} dcm^{-1}) = 297 (1535), 246 (10108), 214 (16574) nm. MS (70 eV): *m*/*z* (%) = 230 (32) $[\mathrm{M}]^+$, 186 (26) $[\mathrm{C_8H_{10}OS_2}]^+$, 167 (35) $[\mathrm{C_9H_{11}OS}]^+$, 153 (100) $[\mathrm{C_8H_9OS}]^+$. $\mathrm{C_{10}H_{14}O_2S_2}$ (230.34): calcd. C 52.14, H 6.13, S 27.84; found C 52.10, H 6.10, S 27.75.

1,2-Bis(2-methoxyethylthio)benzene (4): Yield: 2.34 g (95%); R_f = 0.93 ($\mathrm{CHCl_3}$); $n_\mathrm{D}{}^{20}$ = 1.583. ^{1}H NMR (300 MHz, $\mathrm{CDCl_3}$, 25 °C, $\mathrm{Me_4Si}$): δ = 7.31–7.36 (m, 2 H, $\mathrm{CHC}H\mathrm{CS}$), 7.13–7.19 (m, 2 H, $\mathrm{CHC}H\mathrm{CH}$), 3.59 [t, ^3J(H,H) = 6.8 Hz, 4 H, $\mathrm{CH_2C}H_2\mathrm{O}$], 3.37 (s, 6 H, $\mathrm{OC}H_3$), 3.11 [t, ^3J(H,H) = 6.8 Hz, 4 H, $\mathrm{SC}H_2\mathrm{CH_2}$] ppm. ^{13}C NMR (75 MHz, $\mathrm{CDCl_3}$, 25 °C, $\mathrm{Me_4Si}$): δ = 136.9 ($\mathrm{CH}C\mathrm{S}$), 129.5 ($\mathrm{CH}C\mathrm{HCS}$), 126.6 ($\mathrm{CH}C\mathrm{HCH}$), 70.9 ($\mathrm{CH_2}C\mathrm{H_2O}$), 58.7 ($\mathrm{O}C\mathrm{H_3}$), 32.7 ($\mathrm{S}C\mathrm{H_2CH_2}$) ppm. IR (KBr): $\tilde{\nu}$ = 2980 (C–H), 2925 (C–H), 2877 (C–H), 2824 (C–H), 2808 (C–H), 1446 (C–C), 1114 (C–O), 1094 (C–O), 1042 (C–O) cm^{-1}. UV/Vis ($\mathrm{H_2O}$): $\lambda_{(\mathrm{max})}$ (ε, mol^{-1} dcm^{-1}) = 300 (1310), 247 (9203), 214 (15695) nm. MS (70 eV): *m*/*z* (%) = 258 (44) $[\mathrm{M}]^+$, 200 (54) $[\mathrm{C_9H_{12}OS_2}]^+$, 167 (60) $[\mathrm{C_9H_{11}OS}]^+$, 153 (100) $[\mathrm{C_8H_9OS}]^+$. $\mathrm{C_{10}H_{14}O_2S_2}$ (230.34): calcd. C 55.78, H 7.02, S 24.81; found C 55.68, H 6.99, S 24.92.

General Procedure for the Synthesis of 5 and 6: A suspension of disodium (*Z*)-dicyanoethene-1,2-dithiolate (45 mmol) and a spatula tip of sodium iodide in acetone (80 mL) was heated. 2-Bromoethanol or 2-chloroethyl methyl ether (91 mmol) was added. The suspension was heated under reflux and stirred for 20 h. The precipitate was removed, and the solvent was evaporated. The residue was dissolved in chloroform and washed with water. The organic layer was dried with anhydrous $\mathrm{MgSO_4}$, and the solvents evaporated to dryness to yield a yellow solid, which was purified by recrystallisation from diethyl ether to afford **5** as light brownish and **6** as colourless crystals.

(*Z*)-1,2-Bis(2-hydroxyethylthio)ethene-1,2-dicarbonitrile (5): Yield: 0.94 g (43%); R_f = 0.03 ($\mathrm{CHCl_3}$); m.p. 67.5–68.5 °C. ^{1}H NMR (300 MHz, $\mathrm{CDCl_3}$, 25 °C, $\mathrm{Me_4Si}$): δ = 3.92 [t, ^3J(H,H) = 5.7 Hz, 4 H, $\mathrm{CH_2C}H_2\mathrm{O}$], 3.32 [t, ^3J(H,H) = 5.7 Hz, 4 H, $\mathrm{SC}H_2\mathrm{CH_2}$], 2.04 (s, 2 H, $\mathrm{O}H$) ppm. ^{13}C NMR (75 MHz, $\mathrm{CDCl_3}$, 25 °C, $\mathrm{Me_4Si}$): δ = 121.8 ($\mathrm{C{=}}C$), 112.2 (CN), 61.3 ($\mathrm{CH_2}C\mathrm{H_2O}$), 37.8 ($\mathrm{S}C\mathrm{H_2CH_2}$) ppm. IR (KBr): $\tilde{\nu}$ = 3325 (O–H), 2210 (C≡N), 2001 (C≡N), 1492 (C=C), 1061 (C–OH), 1014 (C–OH), 999 (C–OH) cm^{-1}. UV/Vis ($\mathrm{H_2O}$): $\lambda_{(\mathrm{max})}$ (ε, mol^{-1} dcm^{-1}) = 341 (13902), 275 (4450), 216 (5896) nm. MS (70 eV): *m*/*z* (%) = 230 (20) $[\mathrm{M}]^+$, 169 (13) $[\mathrm{C_6H_5N_2S_2}]^+$, 159 (19) $[\mathrm{C5H5NOS_2}]^+$, 45 (100) $[\mathrm{C_2H_5O}]^+$. $\mathrm{C_8H_{10}N_2O_2S_2}$ (230.30): calcd. C 41.72, H 4.38, N 12.16, S 27.84; found C 41.81, H 4.32, N 12.21, S 27.79.

(*Z*)-1,2-Bis(2-methoxyethylthio)ethene-1,2-dicarbonitrile (6): Yield: 0.76 g (31%); R_f = 0.660 ($\mathrm{CHCl_3}$); m.p. 36.3–37.2 °C. ^{1}H NMR (300 MHz, $\mathrm{CDCl_3}$, 25 °C, $\mathrm{Me_4Si}$): δ = 3.66 [t, ^3J(H,H) = 5.9 Hz, 4 H, $\mathrm{CH_2C}H_2\mathrm{O}$], 3.39 (s, 6 H, $\mathrm{OC}H_3$), 3.32 [t, ^3J(H,H) = 5.9 Hz, 4 H, $\mathrm{SC}H_2\mathrm{CH_2}$] ppm. ^{13}C NMR (75 MHz, $\mathrm{CDCl_3}$, 25 °C, $\mathrm{Me_4Si}$): δ

= 121.1 (C=*C*), 112.1 (CN), 70.6 (CH$_2$*C*H$_2$O), 59.0 (O*C*H$_3$), 34.8 (S*C*H$_2$CH$_2$) ppm. IR (KBr): ṽ = 2212 (C≡N), 2002 (C≡N), 1504 (C=C), 1109 (C–O), 1040 (C–O) cm^{-1}. UV/Vis (H$_2$O): $\lambda_{(max)}$ (ε, mol^{-1} dcm^{-1}) = 340 (13902), 276 (4255), 215 (5803) nm. MS (70 eV): *m*/*z* (%) = 258 (21) [M]$^+$, 199 (4) [C$_7$H$_7$N$_2$OS$_2$]$^+$, 59 (54) [C$_3$H$_7$O]$^+$, 45 (100) [C$_2$H$_5$O]$^+$. C$_{10}$H$_{14}$N$_2$O$_2$S$_2$ (258.35): calcd. C 46.49, H 5.46, N 10.84, S 24.82; found C 46.55, H 5.49, N 10.93, S 24.85.

General Procedure for the Synthesis of [PdCl$_2$(L)] (L = 1–6): The ligands (0.11 mmol) were dissolved in MeOH (5 mL) and a solution of Na$_2$PdCl$_4$ (0.1 mmol) in MeOH (15 mL) was added. This solution was allowed to stand at 5 °C for 4 d. The orange precipitate formed was collected by filtration and washed with MeOH. The single crystals of the complexes that occurred in the (*R*,*S*)-form were prism-shaped, whereas those that occurred as a racemate were needle-shaped.

Dichlorido[1,2-bis(2-hydroxyethylthio)-4-methylbenzene]palladium(II) [PdCl$_2$(1)]: Yield: 0.20 g (47%); m.p. 163.0–164.7 °C. IR (KBr): ṽ = 3474 (O–H), 3428 (O–H), 1070 (C–OH), 1020 (C–OH), 1005 (C–OH) cm^{-1}. FIR (ATR): ṽ = 325 (Pd–Cl) cm^{-1}. HRMS (ESI): calcd. for C$_{11}$H$_{16}$ClO$_2$PdS$_2$ [M – Cl]$^+$ 374.9310, 386.9304; found 384.9304, 386.9293. C$_{11}$H$_{16}$Cl$_2$O$_2$PdS$_2$ (421.67): calcd. C 31.33, H 3.82, Pd 25.24, S 15.21; found C 31.42, H 3.82, Pd 25.14, S 15.34.

Dichlorido[1,2-bis(2-methoxyethylthio)-4-methylbenzene]palladium(II) [PdCl$_2$(2)]: Yield: 0.23 g (52%); m.p. 113.3–115.5 °C. IR (KBr): ṽ = 1114 (C–O), 1097 (C–O), 1043 (C–O) cm^{-1}. FIR (ATR): ṽ = 326 (Pd–Cl) cm^{-1}. HRMS (ESI): calcd. for C$_{13}$H$_{20}$Cl$_2$O$_2$PdS$_2$Na [M + Na]$^+$ 470.9208, 472.9198; found 470.9211, 472.9201; calcd. for C$_{13}$H$_{20}$ClO$_2$PdS$_2$ [M – Cl]$^+$ 412.9624, 414.9617; found 412.9629, 414.9624. C$_{13}$H$_{20}$Cl$_2$O$_2$PdS$_2$ (449.73): calcd. C 34.72, H 4.48, Pd 23.66, S 14.26; found C 34.87, H 4.41, Pd 23.96, S 14.22.

Dichlorido[1,2-bis(2-hydroxyethylthio)benzene]palladium(II) [PdCl$_2$(3)]: Yield: 0.30 g (73%); m.p. 199.5 (needles), 203.5 °C (prisms). IR (KBr): (needles) ṽ = 3387 (O–H), 3347 (O–H), 1077 (C–OH), 1052 (C–OH), 1012 (C–OH), 1005 (C–OH) cm^{-1}. IR (KBr): (prisms) ṽ = 3452 (O–H), 1073 (C–OH), 1066 (C–OH), 1020 (C–OH), 1006(C–OH). FIR (ATR): (needles) ṽ = 321 cm^{-1} (Pd–Cl); FIR (ATR): (prisms) ṽ = 326 cm^{-1} (Pd–Cl). HRMS (ESI): calcd. for C$_{10}$H$_{14}$ClO$_2$PdS$_2$ [M – Cl]$^+$ 370.9153, 372.9147; found 370.9155, 372.9141. C$_{10}$H$_{14}$Cl$_2$O$_2$PdS$_2$ (407.65): calcd. C 29.46, H 3.46, Pd 26.10, S 15.73; found C 29.39, H 3.43, Pd 26.11, S 15.63.

Dichlorido[1,2-bis(2-methoxyethylthio)benzene]palladium(II) [PdCl$_2$(4)]: Yield: 0.26 g (60%); m.p. 174.2–176.5 °C. IR (KBr): ṽ = 1116 (C–O), 1096 (C–O), 1042 (C–O) cm^{-1}. FIR (ATR): ṽ = 320 cm^{-1} (Pd–Cl). HRMS (ESI): calcd. for C$_{12}$H$_{18}$ClO$_2$PdS$_2$ [M – Cl]$^+$ 398.9467, 400.9460; found 398.9478, 400.9472. C$_{12}$H$_{18}$Cl$_2$O$_2$PdS$_2$ (435.70): calcd. C 33.08, H 4.16, Pd 24.42, S 14.72; found C 33.22, H 4.11, Pd 24.27, S 14.65.

Dichlorido[(*Z*)-1,2-bis(2-methoxyethylthio)-1,2-dicyanoethene]palladium(II) [PdCl$_2$(6)]: Yield: 0.27 g (63%); m.p. 141.0–148.0 °C. IR (KBr): ṽ = 2233 (C≡N), 1566 (C=C), 1114 (C–O), 1075 (C–O) cm^{-1}. FIR (ATR): ṽ = 325 cm^{-1} (Pd–Cl). HRMS (ESI): calcd. for C$_{10}$H$_{13}$Cl$_3$N$_2$O$_2$Pd$_2$S$_2$ [M – H$^+$+ Cl$^-$+Pd^{2+}+e$^-$]$^-$ 577.7546; found 577.7653. C$_{10}$H$_{14}$Cl$_2$N$_2$O$_2$PdS$_2$ (435.66): calcd. C 27.57, H 3.24, N 6.43, Pd 24.43, S 14.72; found C 27.80, H 3.30, N 6.38, Pd 24.23, S 14.60.

X-ray Structure Determination and Refinement: Suitable crystals for single-crystal X-ray diffraction were mounted on a glass fibre and placed in the cryosystem of the diffractometer. Crystals of **5**, **6**,

Table 4. Crystal data and structure refinement for **3**, **5** and **6**.

	3	5	6
Empirical formula	C$_{10}$H$_{14}$O$_2$S$_2$	C$_8$H$_{10}$N$_2$O$_2$S$_2$	C$_{10}$H$_{14}$N$_2$O$_2$S$_2$
M [g mol^{-1}]	230.33	230.30	258.35
Crystal description	needle	needle	block
Crystal colour	colourless	colourless	colourless
Crystal size [mm]	1.30. 0.29. 0.21	1.00. 0.40. 0.10	0.500. 0.347. 0.240
Crystal system	orthorhombic	monoclinic	triclinic
Space group	$P2_12_12_1$	$C2/c$	$P\bar{1}$
Unit cell dimensions			
a [Å]	8.7515(10)	23.290(3)	7.9106(15)
b [Å]	9.5547(16)	4.8885(2)	8.5343(17)
c [Å]	12.8493(17)	21.742(2)	10.803(2)
a [°]	90	90	97.441(16)
b [°]	90	121.683(8)	100.640(15)
γ [°]	90	90	113.250(15)
V [Å]	1074.4(3)	2106.4(3)	641.8(2)
Z	4	8	2
$\rho_{calcd.}$ [g cm^{-3}]	1.424	1.452	1.337
F (000)	488	960	272
μ [mm^{-1}]	0.466	0.481	0.403
$T_{max.}/T_{min.}$	0.8308/0.8298	0.7924/0.5261	0.8843/0.8852
2 $\theta_{max.}$ (°)	50.26	50.00	50.00
Collected reflections	6884	9388	4207
Independent reflections	1906	1836	2133
R_{int}	0.0682	0.0621	0.0580
Reflections with $I > 2\sigma(I)$	1704	1682	1506
Parameters	134	157	146
R_1/wR_2 [$I > 2\sigma(I)$]	0.0307/0.0698	0.0490/0.1214	0.0370/0.0870
R_1/wR_2 [all data]	0.0348/0.0713	0.0528/0.1240	0.0545/0.0911
Min./max. $\Delta\rho$ [10^{-6} e pm^{-3}]	–0.270/0.166	–0.328/0.484	–0.336/0.207
GooF	0.972	1.133	0.895

Table 5. Crystal data and structure refinement for the palladium complexes.

	[PdCl$_2$(**1**)][a]	[PdCl$_2$(**2**)][a]	[PdCl$_2$(**3**)][a]	[PdCl$_2$(**3**)][b]	[PdCl$_2$(**4**)][b]	[PdCl$_2$(**6**)][b]
Empirical formula	$C_{11}H_{16}Cl_2O_2PdS_2$	$C_{13}H_{20}Cl_2O_2PdS_2$	$C_{10}H_{14}Cl_2O_2PdS_2$	$C_{10}H_{14}Cl_2O_2PdS_2$	$C_{12}H_{18}Cl_2O_2PdS_2$	$C_{10}H_{14}Cl_2N_2O_2PdS_2$
M [g mol^{-1}]	421.66	449.71	407.63	407.63	435.68	435.65
Crystal description	prism	block	prism	needle	needle	needle
Crystal colour	orange	orange	orange	orange	yellow	brown
Crystal size [mm]	0.500×0.325×0.175	0.340×0.253×0.190	0.400×0.350×0.260	0.900×0.338×0.040	1.100×0.457×0.110	1.64×0.11×0.05
Crystal system	monoclinic	monoclinic	monoclinic	monoclinic	monoclinic	monoclinic
Space group	$P2_1/n$	$P2_1/c$	$P2_1/n$	$P2_1/c$	Cc	$P2_1/c$
Unit cell dimensions						
a [Å]	7.9338(7)	11.3469(5)	8.0445(6)	8.6545(12)	10.6170(12)	12.0070(18)
b [Å]	15.8975(11)	11.2729(3)	14.1803(9)	19.1338(19)	23.048(2)	7.5194(7)
c [Å]	12.1618(12)	14.6773(7)	12.5617(10)	8.4479(11)	8.5484(10)	17.959(3)
a [°]	90	90	90	90	90	90
b [°]	101.248(7)	111.894(3)	103.541(6)	103.469(11)	128.125(8)	108.651(11)
γ [°]	90	90	90	90	90	90
V [Å^3]	1504.5(2)	1742.00(12)	1393.12(18)	1360.4(3)	1645.5(3)	1536.3(4)
Z	4	4	4	4	4	4
ρ calcd. [g cm^{-3}]	1.862	1.715	1.944	1.990	1.759	1.884
F(000)	840	904	808	808	872	864
μ [mm^{-1}]	1.856	1.609	2.001	2.049	1.700	1.825
$T_{max.}/T_{min.}$	0.6090/0.6035	0.8136/0.5766	0.5429/0.5351	0.7702/0.7684	0.6621/0.6580	0.7762/0.7745
2 $\theta_{max.}$ [°]	58.82	50.00	50.00	50.00	55.00	58.90
Collected reflections	12184	21912	8893	8706	6827	9461
Indep. reflections	3447	3057	2454	2396	3537	2699
R_{int}	0.0589	0.0568	0.0472	0.0635	0.0328	0.0628
Reflections with $I > 2\sigma(I)$	3138	2752	2264	1979	3400	2246
Parameters	167	182	197	161	191	196
R_1/wR_2 [$I > 2\sigma(I)$]	0.0425/0.1100	0.0523/0.1108	0.0191/0.0472	0.0241/0.0511	0.0254/0.0650	0.0352/0.0732
R_1/wR_2 [all data]	0.0461/0.1120	0.0576/0.1129	0.0218/0.0481	0.0333/0.0529	0.0264/0.0653	0.0466/0.0759
Min./max. $\Delta\rho$ [10^{-6} e pm^{-3}]	–1.240/0.796	–0.883/0.879	–0.493/0.513	–0.753/0.794	–0.591/0.495	–0.668/1.663
GooF	1.082	1.209	1.035	0.955	1.046	1.032

[a] (*R*,*S*)-configuration of the sulfur atoms. [b] (*R*,*R*) and (*S*,*S*)-configuration of the sulfur atoms.

(*R*,*S*)-[PdCl$_2$(**2**)] and (*R*,*R*;*S*,*S*)-[PdCl$_2$(**3**)] were selected under perfluoroether oil (perfluoropolyalkyl ether, viscosity 1600 cSt). The X-ray data were collected with an Imaging Plate Diffraction System IPDS-2 (STOE) at 210 K with graphite-monochromated Mo-K_α radiation (λ = 0.71073 Å). Spherical absorption corrections were applied for **3**, **6**, (*R*,*S*)-[PdCl$_2$(**1**)], (*R*,*S*)-[PdCl$_2$(**3**)] and (*R*,*R*;*S*,*S*)-[PdCl$_2$(**3**)], (*R*,*R*;*S*,*S*)-[PdCl$_2$(**4**)] and (*R*,*R*;*S*,*S*)-[PdCl$_2$(**6**)]. A numerical absorption correction was performed for **5** and (*R*,*S*)-[PdCl$_2$(**2**)]. The structures were solved by direct methods using the program SHELXS[33] and refined against F^2 with full-matrix least-squares techniques using the program SHELXL-97.[34] All non-hydrogen atoms were refined anisotropically. In (*R*,*R*;*S*,*S*)-[PdCl$_2$(**4**)], two atoms (O2, C5) were disordered, exhibiting two split positions with occupancies of 70 and 30%. The hydrogen atoms of the hydroxy groups in all structures, and the carbon-bound hydrogen atoms in **5**, (*R*,*S*)-[PdCl$_2$(**3**)] and (*R*,*R*;*S*,*S*)-[PdCl$_2$(**6**)] were localised from difference Fourier maps, the U_{iso}(H) values were set to 1.2 U_{eq}(C,O) or 1.5 $U_{eq}(C_{methyl})$. The carbon hydrogen atoms in **3**, **6**, (*R*,*S*)-[PdCl$_2$(**1**)], (*R*,*S*)-[PdCl$_2$(**2**)], (*R*,*R*;*S*,*S*)-[PdCl$_2$(**3**)] and (*R*,*R*;*S*,*S*)-[PdCl$_2$(**4**)], as well as the hydrogen atoms of the methyl groups [C(5)H$_3$ and C(8)H$_3$] in (*R*,*R*;*S*,*S*)-[PdCl$_2$(**6**)] were calculated in their expected positions and refined using a riding model with *d*(C–H) = 0.93 Å (aromatic), 0.97 Å (methylene) or 0.96 Å (methyl) and U_{iso}(H) = 1.2 $U_{eq}(C_{ar},C_{methylene})$ or U_{iso}(H) = 1.5 $U_{eq}(C_{methyl})$. Intermolecular hydrogen bonds appear in the crystal structures of [PdCl$_2$(**1**)] and [PdCl$_2$(**3**)]. To visualise the structures, the graphic program ORTEP[35] was used. Experimental details and the crystallographic data are reported in Table 4 for the ligands, and Table 5 for [PdCl$_2$(L)].

CCDC-834567 (for **3**), -834562 (for **5**), -834568 (for **6**), -834566 {for (*R*,*S*)-[PdCl$_2$(**1**)]}, -834564 {for (*R*,*S*)-[PdCl$_2$(**2**)]}, -834565 {for (*R*,*S*)-[PdCl$_2$(**3**)]}, -834569 {for (*R*,*R*;*S*,*S*)-[PdCl$_2$(**3**)]}, -834563 {for (*R*,*R*;*S*,*S*)-[PdCl$_2$(**4**)]} and -834570 {for (*R*,*R*;*S*,*S*)-[PdCl$_2$(**6**)]} contain the supplementary crystallographic data for this paper. These data can be obtained free of charge from The Cambridge Crystallographic Data Centre via www.ccdc.cam.ac.uk/data_request/cif.

Voltammetric Measurements: Electrochemical measurements were performed with a PGSTAT302N electrochemical analyser (Metrohm) and cell stand C2 (Bioanalytical Systems) using a platinum disc working electrode (2 mm^2), a platinum wire auxiliary electrode and an anhydrous Ag/Ag$^+$ reference electrode. The experiments were performed using degassed MeCN solutions with 0.1 M [nBu$_4$N][PF$_6$] as the supporting electrolyte at a scan rate of 100 mV/s, and the ferrocene/ferrocinium couple as an internal reference. All potentials are given vs. Fc/Fc$^+$ = 85 mV, peak separation 71 mV, ΔI_p = 1.01.

DFT Calculations: All calculations were carried out using the Gaussian09[23] programme package. We used the LANL2DZ[24] basis set and the CAM-B3LYP[24] functional. For **3**, **6** and [PdCl$_2$(**3**)], geometry optimisation was carried out starting from the experimental crystal structure. For the optimised geometries, ESP-derived charges were calculated according to the Merz–Singh–Kollman scheme,[36] where an atomic radius of 1.63 Å was used for Pd. The same set of calculations was carried out for the corresponding cations of all three compounds. For **3**, also excited state energies and the respective oscillator strength were obtained by the time-dependent DFT[37] approach using the same functional and basis set.

NMR Experiments on [PdCl$_2$(2)] and [PdCl$_2$(4)]: The measurements were performed with a Bruker AVANCE 600 spectrometer operating at ^{1}H and ^{13}C frequencies of 600.24 and 150.94 MHz, respectively. All spectra were recorded and processed using BRUKER standard software (TOPSPIN 2.1). Typical numbers of scans were 16 for ^{1}H and 1024 for ^{13}C NMR spectra. For low-temperature measurements, a BVT 3200 variable-temperature unit was used. The internal thermocouple was calibrated using an external Pt100 thermocouple, which was applied at the same position in the probe where the sample (NMR tube) is usually located. The chemical shifts are reported relative to the solvent signal of dichloromethane: ^{1}H NMR $\delta(^1\text{H})$ = 5.31 ppm and ^{13}C NMR $\delta(^{13}\text{C})$ = 53.7 ppm. The other complexes were not soluble enough to give spectra worthy of evaluation.

Determination of the Complex Stability Constants: The UV/Vis spectra were recorded with a Perkin–Elmer Lambda 950 spectrophotometer using sealed quartz cuvettes. Titrations were carried out starting with **1**–**6** (2 mL, $c = 5\times10^{-5}$ M) and adding palladium solutions (1000 ppm palladium absorption standard solution in 5% w/w HCl from Sigma–Aldrich diluted to $c = 5\times10^{-4}$ M) in 10 µL steps every 5 minutes with a Metrohm 805 Dosimat connected to a 846 Dosing Interface. Deionised water (Elga, Purelab ultra) was used as the solvent.

Solvent Extraction Experiments and ICP OES: All solvent extraction batch experiments were carried out at room temperature. Equal volumes of the aqueous and organic (10^{-2} M ligand in CHCl$_3$ uvasol from Merck) phases were mixed with a Heidolph Multi Reax vibrating shaker (ca. 1900 rpm) and separated by centrifugation. The metal content of the aqueous phase was determined before and after the extraction with an Optima 5300 DV ICP OES from Perkin–Elmer. To prepare the model solutions, a 1000 ppm palladium absorption standard solution in 5% (w/w) HCl from Sigma–Aldrich and 30% (w/w) suprapur hydrochloric acid from Merck were diluted. The solution of the automotive catalyst was obtained by leaching the monolith (1 kg) with heating with aqua regia (2 L) until the evolution of the gas was finished. Afterwards it was diluted with the same volume of deionised water (Elga, Purelab ultra). The oxidation potential of this solution was 1.05 V (vs. SHE). For the measurement of the organic samples, it was necessary to mix chloroform with water with the help acetic acid to obtain one phase. In this way it was possible to use an aqueous stock solution to prepare the standards and carry out the calibration in the same matrix as the samples. On this account, the organic (1.5 mL, sample or pure CHCl$_3$) was added to the aqueous solution (1.5 mL, pure water or aqueous standard solution respectively) and mixed with suprapur glacial acetic acid (7 mL, Merck). This was measured using a GemCone nebuliser and a baffled cyclonic spray chamber. The measurement of the aqueous samples was performed with a cross-flow nebuliser and a Ryton Scott spray chamber.

Supporting Information (see footnote on the first page of this article): Scheme for the attribution of the NMR resonances of **1**–**4**, additional crystallographic data and all X-ray structures, more information about orbitals, ESP charges and excited states, NMR spectra and data for the complexes, calculation of the complex stability constants, UV/Vis absorption spectra and titration curves of **1**, **2** and **4**, list of wavelengths chosen for the determination of the metal content by ICP OES.

Acknowledgments

We thank the Arbeitsgemeinschaft industrieller Forschungsvereinigungen "Otto von Guericke" e.V. (AIF) and ReMetall Drochow GmbH for financial support and Cognis for the supply of Aloxime® 840. Special thanks are due to Dr. Christine Fischer (Leibniz Institute for Catalysis, University of Rostock) for MS measurements, Sigrid Imme (Technische Universität Berlin), and Sylvia Pirok (Max Planck Institute of Colloids and Interfaces) for the elementary analyses of the palladium complexes.

---

[1] C. Hagelüken, M. Buchert, H. Stahl, in: *Stoffströme der Platingruppenmetalle* (Ed.: C. Hagelüken), GDMB Medienverlag, Clausthal-Zellerfeld, Germany, **2005**, pp. 1–16.
[2] F. Bernardis, R. A. Grant, D. C. Sherrington, *React. Funct. Polym.* **2005**, *65*, 205–217.
[3] G. P. Demopoulos, *Can. Min. Metall. Bull.* **1989**, *82*, 165–171.
[4] M. J. Cleare, R. A. Grant, P. Charlesworth, *Extr. Metall. 81, Pap. Symp.* **1981**, *5*, 34–41.
[5] a) V. V. Yakshin, O. M. Vilkova, I. G. Tananaev, B. F. Myasoedov, *Russ. J. Gen. Chem.* **2011**, *81*, 1966–1971; b) S. Katsuta, Y. Yoshimoto, M. Okai, Y. Takeda, K. Bessho, *Ind. Eng. Chem. Res.* **2011**, *50*, 12735–12740; c) A. Cieszynska, M. Wisniewski, *Sep. Purif. Technol.* **2011**, *80*, 385–389; d) Y. Baba, Y. Kanai, S. Kanemaru, T. Oshima, *Solvent Extr. Res. Dev. Jpn.* **2010**, *17*, 195–207; e) M. Regel-Rosocka, M. Wisniewski, A. Borowiak-Resterna, A. Cieszynska, A. M. Sastre, *Purif. Technol.* **2007**, *53*, 337–341; f) A. N. Turanov, V. K. Karandashev, A. N. Proshin, *Solvent Extr. Ion Exch.* **2008**, *26*, 360–374; g) F. Hamada, C.-B. Li, Y. Kondo, US 20110247459 A1, **2011**; h) S. Feng, Z. Huang, P. Li, *Asian J. Chem.* **2011**, *23*, 2605–2608; i) R. A. Khisamutdinov, G. R. Anpilogova, Y. I. Murinov, L. V. Spirikhin, *Russ. J. Inorg. Chem.* **2010**, *55*, 1992–1997.
[6] S. G. Murray, F. R. Hartley, *Chem. Rev.* **1981**, *81*, 365–414 and references therein.
[7] F. R. Hartley, S. G. Murray, W. Levason, H. E. Soutter, C. A. McAuliffe, *Inorg. Chim. Acta* **1979**, *35*, 265–277.
[8] V. P. Ananikov, A. O. Piroyan, K. A. Gaiduk, I. P. Beletskaya, V. N. Khrustalev, *Russ. J. Org. Chem.* **2009**, *45*, 1753–1764.
[9] H. Renner, *The selective extraction of palladium by the use of di-n-hexyl sulfide*, Council for Mineral Technology, **1985**, Report No. M217.
[10] H.-J. Drexler, I. Starke, M. Grotjahn, E. Kleinpeter, H.-J. Holdt, *Inorg. Chim. Acta* **2001**, *317*, 133–142, and references cited therein.
[11] H.-J. Holdt, *Pure Appl. Chem.* **1993**, *65*, 477–482.
[12] R. Heber, *J. Prakt. Chem.* **1976**, *318*, 19–25.
[13] E. W. Abel, S. K. Bhargava, K. Kite, K. G. Orrell, V. Šik, B. L. Williams, *Polyhedron* **1982**, *1*, 289–298.
[14] K. C. Sole, in: *Solvent Extraction and Liquid Membranes* (Eds.: M. Aguilar, J. L. Cortina), Taylor & Francis Group, Boca Raton, **2008**, pp. 175–176.
[15] S. F. Woollam, R. A. Grant, *Proceedings of ISEC 2008* **2008**, 281–286.
[16] M. Giolando, K. Kirschbaum, *Synthesis* **1992**, *5*, 451–452.
[17] D. G. Bähr, G. Schleitzer, *Chem. Ber.* **1957**, *90*, 438–443.
[18] S. J. Lange, J. W. Sibert, C. L. Stern, A. G. M. Barrett, B. M. Hoffman, *Tetrahedron* **1995**, *51*, 8175–8188.
[19] See the Supporting Information for additional crystallographic data and all X-ray structures, more information about orbitals, ESP charges and excited states, NMR spectra and data of the complexes, calculation of the complex stability constants, UV/Vis absorption spectra and titration curves of **1**, **2** and **4** and a list of wavelengths chosen for the determination of the metal content by ICP OES.
[20] a) M. Dräger, G. Kiel, G. Gattow, *Chem. Ber.* **1973**, *106*, 3929–3937; b) R. D. Calleja, E. S. Martinez, S. Friederichs, J. Kudnig, J. Bracker, G. Klar, *J. Mater. Chem.* **1995**, *5*, 389–394.

[21] a) L. R. Gray, D. J. Gulliver, W. Levason, M. Webster, *Acta Crystallogr., Sect. C: Cryst. Struct. Commun.* **1983**, *39*, 877–879; b) N. Takeda, D. Shimizu, N. Tokitoh, *Inorg. Chem.* **2005**, *44*, 8561–8568; c) N. Takeda, D. Shimizu, T. Sasamori, N. Tokitoh, *Acta Crystallogr., Sect. E. Struct. Rep. Online* **2005**, *61*, m1408–m1410.

[22] a) M. Tiecco, M. Tingoli, L. Testaferri, D. Chianelli, F. Maiolo, *Synthesis* **1982**, *6*, 478–480; b) M. Tiecco, L. Testaferri, M. Tingoli, D. Chianelli, M. Montanucci, *J. Org. Chem.* **1983**, *48*, 4795–4800; c) M. V. Ramana Reddy, S. Reddy, P. V. Ramana Reddy, D. Bhaskar Reddy, N. Subba Reddy, *Phosphorus Sulfur Silicon Relat. Elem.* **1989**, *44*, 123–127; d) B. Tylleman, G. Gbabode, C. Amato, C. Buess-Herman, V. Lemaur, J. Cornil, R. G. Aspe, Y. H. Geerts, S. Sergeyev, *Chem. Mater.* **2009**, *21*, 2789–2797.

[23] M. J. Frisch, G. W. Trucks, H. B. Schlegel, G. E. Scuseria, M. A. Robb, J. R. Cheeseman, G. Scalmani, V. Barone, B. Mennucci, G. A. Petersson, H. Nakatsuji, M. Caricato, X. Li, H. P. Hratchian, A. F. Izmaylov, J. Bloino, G. Zheng, J. L. Sonnenberg, M. Hada, M. Ehara, K. Toyota, R. Fukuda, J. Hasegawa, M. Ishida, T. Nakajima, Y. Honda, O. Kitao, H. Nakai, T. Vreven, J. A. Montgomery Jr, J. E. Peralta, F. Ogliaro, M. Bearpark, J. J. Heyd, E. Brothers, K. N. Kudin, V. N. Staroverov, R. Kobayashi, J. Normand, K. Raghavachari, A. Rendell, J. C. Burant, S. S. Iyengar, J. Tomasi, M. Cossi, N. Rega, J. M. Millam, M. Klene, J. E. Knox, J. B. Cross, V. Bakken, C. Adamo, J. Jaramillo, R. Gomperts, R. E. Stratmann, O. Yazyev, A. J. Austin, R. Cammi, C. Pomelli, J. W. Ochterski, R. L. Martin, K. Morokuma, V. G. Zakrzewski, G. A. Voth, P. Salvador, J. J. Dannenberg, S. Dapprich, A. D. Daniels, Ö. Farkas, J. B. Foresman, J. V. Ortiz, J. Cioslowski, D. J. Fox, *Gaussian 09*, rev. A.2, Gaussian, Inc., Wallingford CT, **2009**.

[24] T. Yanai, D. Tew, N. Handy, *Chem. Phys. Lett.* **2004**, *393*, 51–57; T. H. Dunning Jr, P. J. Hay, in: *Modern Theoretical Chemistry*, vol. 3 (Ed.: H. F. Schaefer III), Plenum, New York, **1976**, pp. 1–28; P. J. Hay, W. R. Wadt, *J. Chem. Phys.* **1985**, *82*, 270–283.

[25] B. H. Besler, K. M. Merz Jr, P. A. Kollman, *J. Comput. Chem.* **1990**, *11*, 431–439; U. C. Singh, P. A. Kollman, *J. Comput. Chem.* **1984**, *5*, 129–145.

[26] T. Schwarze, H. Müller, C. Dosche, T. Klamroth, W. Mickler, A. Kelling, H.-G. Löhmannsröben, P. Saalfrank, H.-J. Holdt, *Angew. Chem.* **2007**, *119*, 1701; *Angew. Chem. Int. Ed.* **2007**, *46*, 1671–1674.

[27] A. F. Holleman, E. Wiberg, in: *Lehrbuch der Anorganischen Chemie* (Ed.: N. Wiberg), 34th ed., appendix IV, de Gruyter, Berlin, **1995**.

[28] S. Rizzato, J. Bergès, S. A. Mason, A. Albinati, J. Kozelka, *Angew. Chem. Int. Ed.* **2010**, *49*, 7440–7443.

[29] E. W. Abel, R. P. Bush, F. J. Hopton, C. R. Jenkins, *Chem. Commun. (London)* **1966**, *3*, 58–59.

[30] H.-J. Holdt, H. Müller, A. Kelling, H.-J. Drexler, T. Müller, T. Schwarze, U. Schilde, I. Starke, *Z. Anorg. Allg. Chem.* **2006**, *623*, 114–122.

[31] L. I. Elding, *Inorg. Chim. Acta* **1972**, *6*, 647–651.

[32] H.-J. Holdt, J. Teller, *Z. Chem.* **1988**, *7*, 249–250.

[33] G. M. Sheldrick, *SHELXS-97*. *Program for Crystal Structure Solution*, Göttingen, **1997**.

[34] G. M. Sheldrick, *SHELXL-97*. *Program for Crystal Structure Refinement*, Göttingen, **1997**.

[35] ORTEP3 for Microsoft Windows®, v. 2.02: L. J. Farrugia, *J. Appl. Crystallogr.* **1997**, *30*, 565–565.

[36] B. H. Besler, K. M. Merz Jr, P. A. Kollman, *J. Comput. Chem.* **1990**, *11*, 431–439; U. C. Singh, P. A. Kollman, *J. Comput. Chem.* **1984**, *5*, 129–145.

[37] M. E. Casida, C. Jamorski, K. C. Casida, D. R. Salahub, *J. Chem. Phys.* **1998**, *108*, 4439–4449.

Received: December 16, 2011